

Geometry Effects on the Formation of the Hydrogen Ly α Line in Planetary Nebulae

A. Peraiah and R. Wehrse

Institut für Theoretische Astrophysik der Universität Heidelberg, Im Neuenheimer Feld 294, D-6900 Heidelberg, Federal Republic of Germany

Received April 4, revised June 6, 1977

Summary. In order to study the effects of sphericity on the radiative transfer in the hydrogen Ly α line of planetary nebulae, the radiation field in this line is calculated for static pure hydrogen models with ratios of outer to inner radii approximately equal to 2, 4 and 8. For $r_{\text{out}}/r_{\text{in}} \approx 2$ the transfer equation is also solved in plane parallel approximation for comparison. Both reflecting and open inner boundaries are considered. The transfer equation has been solved in the framework of the discrete space theory. In the spherical calculations the profiles of the emergent radiation are not found to be very different in their shapes (one from another) while there are large differences in the internal radiation fields. Substantial changes occur for most quantities, when the spherical approximation is replaced by the plane parallel one.

Key words: spherical radiative transfer — hydrogen Ly α — planetary nebulae

I. Introduction

The radiative transfer in the hydrogen Ly α line of gaseous nebulae has been studied by many authors during the last three decades (for a review see Osterbrock, 1974). To our knowledge however, there is only one paper (Panagia and Ranieri, 1972), in which the spherical geometry is taken into account for a static nebula. Panagia and Ranieri solve the transfer equation for a number of optical depths, ratios of outer to inner radius and photon generation functions by means of Monte Carlo techniques assuming a pure hydrogen composition. Graphs of emergent fluxes and mean number of scatterings are shown. As a consequence of the small number of photons considered their results however are rather crude, e.g. they estimate that the errors in the mean number of scatterings may be up to 10%, and the histograms describing the profiles indicate even higher errors.

The intentions of this paper are (i) to present independent calculations on the influence of the

geometry on the emergent fluxes with very high precision (see Section II) and (ii) to give in addition the radial dependence of the total mean intensities, which provides information on the dust heating and center to limb variation in the infrared. In Section II we describe the model and transfer calculations, and the results are given and discussed in Section III.

II. Model and Transfer Calculations

We consider static homogeneous, pure hydrogen nebulae of density $\rho = 10^3 m_{\text{H}} = 1.66 \cdot 10^{-21} \text{ gr/cm}^3$, each being ionized by a central star emitting $S = 10^{45}$ photons/s with $h\nu > 13.6 \text{ eV}$. This corresponds to the emission of a blackbody of temperature $T_{\text{bb}} = 50000 \text{ K}$ and radius $R_{\text{bb}} = 3.5 \cdot 10^9 \text{ cm} = 0.05 R_{\odot}$. The electron temperature is assumed to be $T_e = 10^4 \text{ K}$. The radius of the central hole r_{in} is taken as a free parameter. We determine the ionization structure numerically by means of a program described by Baschek and Wehrse (1975). The outer radii of the nebulae r_{out} are put equal to the Strömgren radius r_s , defined by the distance at which the fractional ionization drops to 0.5. The relevant numbers for the models used in this paper are listed in Table 1. The radial dependence of the ionization degree, which controls both the absorption coefficients and the source function, is shown in Figure 1.

With the data from these models we solve the equation of radiative transfer in the hydrogen Ly α line,

$$\mu \frac{\partial I(x, \mu, r)}{\partial r} + \frac{1-\mu^2}{r} \frac{\partial I(x, \mu, r)}{\partial \mu} = \chi(x, r) \left\{ -I(x, \mu, r) + \int_{-\infty}^{+\infty} \phi(x') J(x') dx' + S(r) \right\}. \quad (1)$$

Here $I(x, \mu, r)$ is the specific intensity at frequency $x [= (v - v_0)/\Delta v_D]$, where Δv_D is the Doppler width] directed at an angle $\cos^{-1} \mu$ with the radius vector r . $J(x, r)$ is the corresponding mean intensity at r , $\chi(x, r)$ the line absorption coefficient, and $S(r)$ represents the generation of photons by recombination at r . For the

Table 1. Characteristic data of the models used

Model	$n_e = 10^3 \text{ cm}^{-3}$	$T_e = 10^4 \text{ K}$	$S = 10^{4.5}$
	ionizing photons/s		
	r_{in} (cm)	r_{out} (cm)	$r_{\text{out}}/r_{\text{in}}$
1	$2.5 \cdot 10^{16}$	$2.1 \cdot 10^{17}$	8.40
2	$5.5 \cdot 10^{16}$	$2.1 \cdot 10^{17}$	3.82
3	$1.0 \cdot 10^{17}$	$2.2 \cdot 10^{17}$	2.20

line profile ϕ we use Voigt functions $\frac{1}{\sqrt{\pi}} H(\alpha, \nu)$ with $\alpha = 4.3 \cdot 10^{-4}$, which corresponds to pure radiation damping. In the scattering integral $\int_{\infty}^{\infty} \phi(x') J(x') dx'$ complete redistribution is assumed. This approximation seemed to be justified in this case, since we will restrict our discussion to the comparison of calculations of the same type. The effects of partial redistribution in spherical geometry will be treated in detail in a forthcoming paper (Peraiah, 1977). The transfer Equation (1) is solved by the formalism described by Grant and Peraiah (1972). 25 radial shells of the same geometrical thickness were used.

As we are considering an optically thick medium, the optical depth τ in each shell is much larger than τ_{crit} [which determines the stability of the solution of the transfer equation and its value is determined by the physical and geometrical characteristics of the medium, see the inequality (3.11) of Peraiah and Grant (1973)]. Consequently we halve the shell n times until $\tau_{\text{subshell}} = 2^{-n} \tau_{\text{shell}} \leq \tau_{\text{crit}}$. The total response functions of reflection and transmission of the shell are calculated by employing the star algorithm (Peraiah and Grant, 1973). For the various integrations, formulae of Gauss-Legendre type were used throughout. We employ 20 points for the frequency integration and 4 directions for the integration over μ .

The accuracy of the program has been checked by considering only scattering in the medium in which case the flux must conserve. When the identity (4.3) of Peraiah and Grant (1973) is satisfied and correct normalization of the profile is achieved, the flux is conserved to the machine accuracy but printed only up to 8 digits. In this case we have considered an open inner boundary.

III. Results and Discussion

In Figure 2a the emitted fluxes are shown for a reflecting inner boundary. The profiles labelled 1, 2 and 3 are calculated for spherical symmetry and correspond to models with ratios of outer to inner radii $r_{\text{out}}/r_{\text{in}} \approx 2, 4$ and 8 resp. (compare Table 1). The dotted profile refers to calculations where the ionization model with $r_{\text{out}}/r_{\text{in}} \approx 2$ is used, but the transfer Equation (1) is solved in the plane parallel approximation. The integrated flux increases in this case, since the emitting volume is larger as a consequence of the neglect of r^2 factors. The figure shows a drastic change in the outgoing fluxes, when the plane-parallel approximation is replaced by the more appropriate spherical one. The differences between the other cases are relatively small. This is mainly due to the rapid change of the curvature factor $q_{\text{out}} = \frac{1}{N} (1 - r_{\text{in}}/r_{\text{out}})$ for $1 \lesssim r_{\text{out}}/r_{\text{in}} \lesssim 2$ (note that $r_{\text{out}}/r_{\text{in}} = 1$ refers to plane parallel geometry) and the much slower one for $r_{\text{out}}/r_{\text{in}} \gtrsim 2$.

It should be noticed that the profiles are also influenced by the differences in the ionization structure, since the distribution of $n_e^2(r)$ controls the generation of photons and $n_{\text{H}}(r)$ determines the optical depth in the line. By the use of our models we were however not able to disentangle the ionization from the radiative transfer effects.

In stellar atmospheres one must consider open inner boundary as the photons leaving the inner

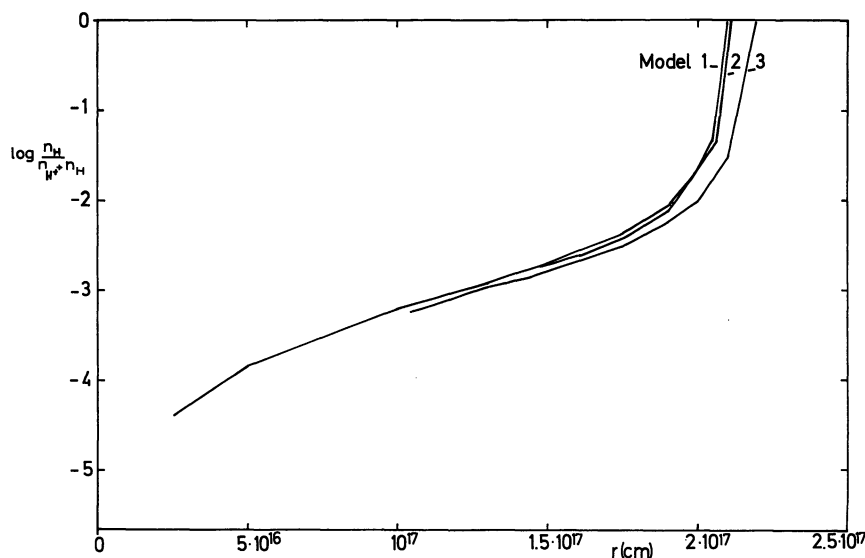


Fig. 1. Radial dependence of the fractional ionization degree $n_{\text{H}}/(n_{\text{H}^+} + n_{\text{H}})$ for the three models considered

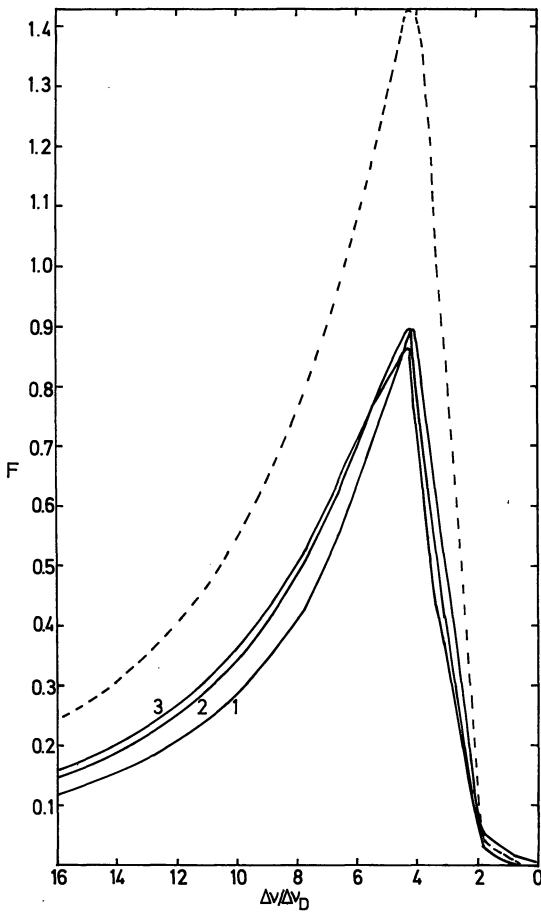


Fig. 2a. Profiles of the emergent fluxes for reflecting inner boundaries. The dotted profile is calculated in plane parallel approximation using the ionization Model No. 1. Since the line is symmetric, only one half is shown

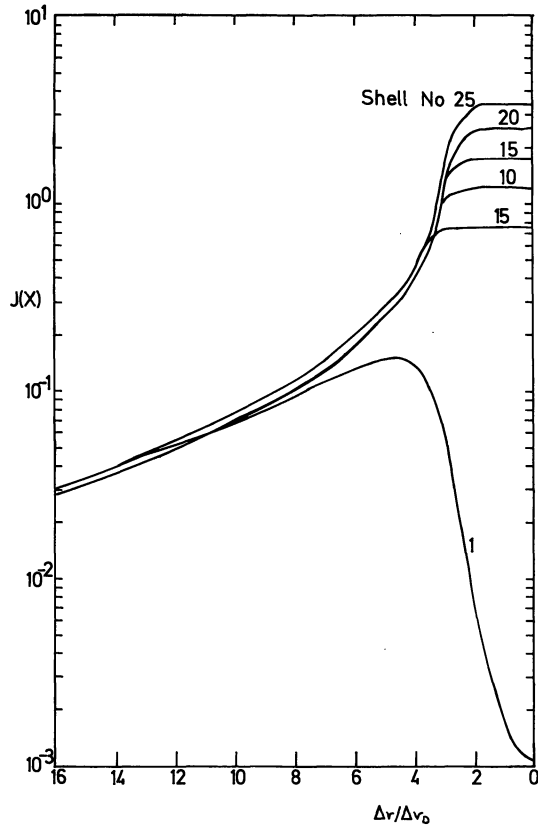


Fig. 3a. Monochromatic mean intensities for some shells within the nebula. The ratio of outer to inner radius is approximately 4 (ionization Model No. 2) and the inner boundary is assumed to be reflecting. The given shell numbers n refer to radial positions $r_n = r_{out} - (r_{out} - r_{in}) * (n - 1) / 25$ (compare text)

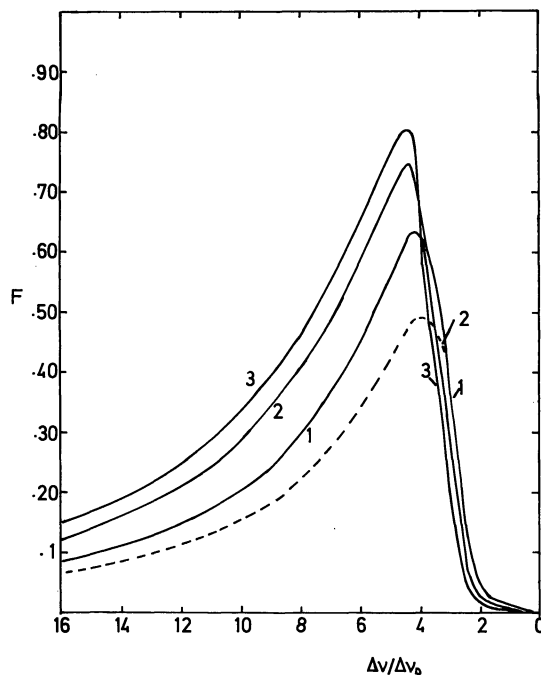


Fig. 2b. Same as Figure 2a for open inner boundaries

boundary enter the star. In planetary nebulae, practically all photons leaving the inner boundary will reenter the nebulae at some other point and therefore it is physically realistic to treat a reflecting inner boundary in the present context. However, it would be interesting to see what fraction of photons leave through the open inner boundary and make a comparison of the emergent profiles obtained with open and totally closed inner boundaries. The corresponding profiles for the open inner boundary are shown in Figure 2b. In all cases the total outgoing flux decreases and it is clearly seen that the fraction of the outgoing flux is increased, when the inner hole is enlarged.

Differences due to changes at the inner boundary show up even clearer in the internal radiation field of the nebula. In Figures 3a and b for $r_{out}/r_{in} \approx 4$ the monochromatic mean intensities are plotted for the two cases and a number of shells. When photons are not allowed to pass the inner edge (Fig. 3a) we have essentially box-type profiles everywhere except at the outer surface, where photons are able to leave even at the line center and therefore a central absorption results. When the inner surface is open, the same phenomenon occurs

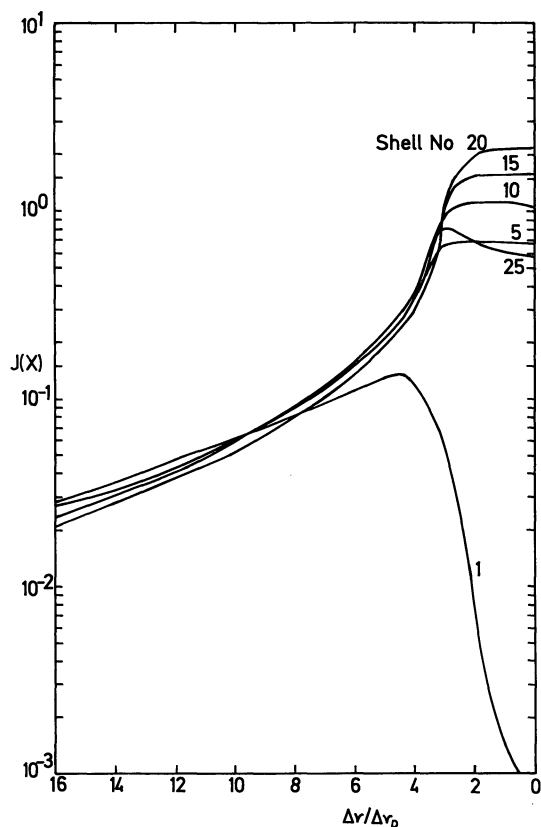


Fig. 3b. Same as Figure 3a for open inner boundary

here, the central absorption is however appreciably weak as a consequence of the peaking effect.

By integrating over the frequency the total mean intensity J is obtained. The radial dependence of J for the models considered here is given in Figures 4a and b. Again the effects of sphericity and inner boundary are clearly seen. The changes of $J(r)$ with $r_{\text{out}}/r_{\text{in}}$ are mainly consequences of different surface areas of the models. Since the calculated nebulae are optically thick and ionized by the same star, the volumes of the H II regions are practically the same, but the surfaces are proportional to $((r_{\text{out}}/r_{\text{in}})^3 - 1)^{2/3} \times ((r_{\text{out}}/r_{\text{in}})^2 + \delta)$, where δ is 0 for reflecting inner boundaries and equals 1 for open inner surfaces. Therefore the intensity has to build up strongest for $r_{\text{out}}/r_{\text{in}} \approx 8$, where the surface is smallest.

For the cases with reflecting inner boundaries it should be noted that the differences of $J(r)$ are larger in the inner parts of the nebulae than at the surfaces and that we always find the maximum of the total mean intensities at the inner edge. The latter is different from the behaviour of the He II Ly α line (Wehrse and Peraiah, 1977), where for spherical calculations a maximum inside was found. We attribute this to the fact that we use here quite different source functions and that no absorption is taken into account in the present calculations.

When the inner boundary is open for the photons I is reduced in every shell. Maxima occur at about

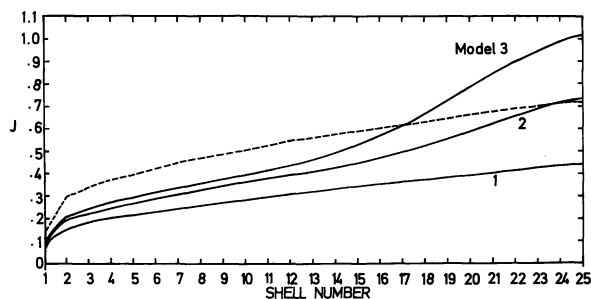


Fig. 4a. The radial distribution (labelled by shell numbers) of the total mean intensities $J(r) = \int_{-\infty}^{\infty} J(x, r) dx$ for calculations with reflecting inner boundaries. The dotted curve gives $J(r)$ for ionization Model 1 and the transfer equation being solved in plane-parallel approximation

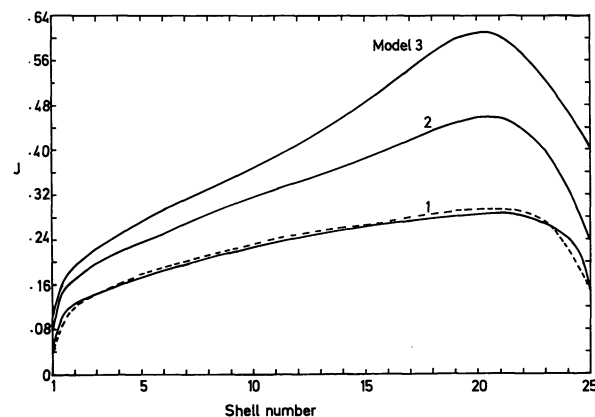


Fig. 4b. Same as Figure 4a for open inner boundary

$r = 1.2 \cdot r_{\text{in}}$. They show that photons inside this radius preferably leave the system via the inner surface.

It should also be remarked that the curves of Figure 4 are interesting in connection with the center to limb variations of planetary nebulae in the infrared, since the dust present in the objects is at least partially heated by the absorption of diffuse Ly α radiation. In this respect the graphs show that in sophisticated models of the infrared emission the on the spot approximation is not adequate (it would give a horizontal line in the figures) and the transfer in the H Ly α line should be properly taken into account.

Acknowledgements. This work has been performed as part of the program of the Sonderforschungsbereich 132 "Theoretische und Praktische Stellarastonomie" which is sponsored by the Deutsche Forschungsgemeinschaft.

References

- Baschek, B., Wehrse, R.: 1975, *Astron. Astrophys.* **43**, 29
- Grant, I. P., Peraiah, A.: 1972, *Monthly Notices Roy. Astron. Soc.* **160**, 239
- Osterbrock, D. E.: 1974, *Astrophysics of Gaseous Nebulae*, W. H. Freeman and Company, San Francisco
- Panagia, N., Ranieri, M.: 1973, *Astron. Astrophys.* **24**, 219
- Peraiah, A., Grant, I. P.: 1973, *J. Inst. Maths. Applics* **12**, 75
- Peraiah, A.: 1977 (to be published)
- Wehrse, R., Peraiah, A.: 1977, submitted to *Astron. Astrophys.*